Ocean carbonate system variability in the North Atlantic Subpolar surface water (1993-2017)

Coraline Leseurre, Claire Lo Monaco, Gilles Reverdin, Nicolas Metzl, Jonathan Fin, Solveig Olafsdottir, Virginie Racapé

Biogeosciences Discuss., https://doi.org/10.5194/bg-2019-119
Manuscript under review for journal Biogeosciences
Discussion started: 5 April 2019

Ocean carbonate system variability in the North Atlantic Subpolar surface water (1993-2017)

Coraline Leseurre[1], Claire Lo Monaco[1], Gilles Reverdin[1], Nicolas Metzl[1], Jonathan Fin[1], Solveig Olafsdottir[2] and Virginie Racapé[3]

[1]Laboratoire d'Océanographie et du Climat : Expérimentation et Approches Numériques (LOCEAN-IPSL), Sorbonne Université-CNRS-IRD-MNHN, Paris, 75005, France
[2] MFRI, Marine and Freshwater Research Institute, Reykjavik, Iceland
[3]Laboratoire d'Océanographie Physique et Spatiale (LOPS), CNRS-IFREMER-IRD-UBO, Plouzané, 29280, France

Correspondence to: Coraline Leseurre (coraline.leseurre1@gmail.com)

Abstract. The North Atlantic is one of the major sinks for anthropogenic CO_2. In this study, we investigate the evolution of CO_2 uptake and ocean acidification in the North Atlantic Subpolar Gyre (50°N-64°N) using repeated observations collected over the last three decades in the framework of the long-term monitoring program SURATLANT (SURveillance de l'ATLANTique). Data obtained between 1993 and 1997 suggest an important reduction in the capacity of the ocean to absorb CO_2 from the atmosphere during summer, due to a rapid increase in the fugacity of CO_2 (fCO_2) in surface waters (5 times faster than the increase in the atmosphere). This was associated with a rapid decrease in surface pH (of the order of -0.014/yr) and was mainly driven by a significant warming and increase in DIC. Similar trends are observed between 2001 and 2007 during both summer and winter with a mean decrease of pH between -0.006/yr and -0.013/yr. These rapid trends are mainly explained by a significant warming of surface waters, a decrease in alkalinity during summer and an increase in DIC during winter. On the contrary, data obtained during the last decade (2008-2017) show a stagnation of surface fCO_2 (increasing the ocean sink for CO_2) and pH. These recent trends are explained by the cooling of surface waters, a small decrease of total alkalinity and the near-stagnation of dissolved inorganic carbon. Overall our results show that the uptake of CO_2 and ocean acidification in the North Atlantic Subpolar Gyre is substantially impacted by multi-decadal variability, in addition to the accumulation of anthropogenic CO_2. As a consequence, the future evolution of air-sea CO_2 fluxes, pH and the saturation state of surface waters with regards to aragonite and calcite remain highly uncertain in this region.

1 Introduction

Observations have shown an increase by more than 40% in atmospheric carbon dioxide (CO_2) since the industrial revolution, resulting in the strengthening of the greenhouse effect (IPCC, 2013 - Hartmann et al., 2013). Despite increasing efforts at the international level to tackle climate change, the last carbon report published by Le Quéré et al. (2018) shows that CO_2 emissions reached 11.3 ± 0.9 GtC in 2017, mainly due to the burning of fossil fuels (9.9 ± 0.5 GtC in 2017, three time higher than in 1960). The ocean plays an important role in climate regulation by absorbing between one quarter and one third of this

anthropogenic carbon (Le Quéré et al., 2018; Gruber et al., 2019). The North Atlantic is known as one of the main anthropogenic CO_2 sinks (Sabine et al., 2004; Khatiwala et al., 2013): this region (north of 50°N), covering 5% of the global surface ocean, is responsible for 20% of the oceanic uptake of anthropogenic CO_2 (Khatiwala et al., 2013), with a mean annual air-sea CO_2 flux estimated at 0.27 PgC/yr (Takahashi et al., 2009). The uptake of CO_2 in the North Atlantic is mainly due to extensive biological activity during summer and considerable heat loss during winter. However, repeated observations have shown important variations in this natural sink for anthropogenic CO_2 in response to climate variability and climate change (Corbière et al., 2007; Metzl et al., 2010; McKinley et al., 2011; Landschützer et al., 2013).

In addition to climate change, CO_2 emissions are responsible for ocean acidification, a phenomenon known as the other CO_2 problem (Doney et al., 2009). Indeed, the accumulation of anthropogenic CO_2 in the ocean has led to a decrease in pH in surface waters by 0.1 unit since the industrial revolution (IPCC, 2013 - Hartmann et al., 2013). Due to the potential threat on marine life, the decrease in pH is recognized as a true indicator of global change, similarly as warming and sea level rise (World Meteorological Organization, 2018). The urgent need for documenting and understanding changes in oceanic pH and its impact on marine life has motivated more studies in recent years. Among them, the data syntheses from Lauvset et al. (2015) and Bates et al. (2014) indicated that pH is decreasing in most of the surface ocean as a result of the increase in oceanic CO_2. In the North Atlantic they reported a decrease ranging between 0.001/yr and 0.003/yr. These estimates were obtained by combining all available data either at fixed monitoring stations in the Iceland Sea, Irminger Sea and offshore Bermuda over the period 1983-2014 (Bates et al., 2014), or in the North Atlantic Subpolar Seasonally Stratified biome over the period 1991-2011 (Lauvset et al., 2015). Here, we use repeated observations collected between Iceland and Newfoundland to investigate further the change in surface pH by evaluating separately summer and winter data, and by taking into account changes in the North Atlantic Subpolar Gyre (NASPG) circulation and water masses (Chafik et al., 2014; Desbruyères et al., 2015; Nigam et al., 2018). This study, based on Total Alkalinity (TA) / Dissolved Inorganic Carbon (DIC) pair observations, allows to evaluate their contribution; while most studies are based on observations of partial pressure of CO_2 (pCO2) and TA/Salinity (Lauvset and Gruber, 2014). The aim of this study is to document the evolution of the CO_2 system parameters in recent years (up to 2017) and to evaluate the drivers for the evolution of surface pH for winter and summer. In this respect, it extends previous analyzes based on SURATLANT observations collected during winter between 1993 and 2008 (Corbière et al., 2007; Metzl et al., 2010).

2 Study area

The NASPG as defined here extends from the east coast of Canada (65°W) to the west coast of Ireland (5°W) mostly north of 50°N. It consists of the Labrador, Irminger and Iceland basins, and the Rockall Plateau and Trough. The NASPG is a region of mixing between subtropical, subpolar and polar surface waters. The inflow of these surface waters is dominated by three surface currents: The North Atlantic Current (NAC), also known in this sector as the North Atlantic Drift, mostly of tropical origin, the East Greenland Current (EGC) and the Labrador Current (LC) which are the conducts to bring waters from further

north and the Arctic (Fig. 1a-b). The North Atlantic Drift delimits the NASPG in the south and transports warm (8°C to 15°C) and salty (35 to 36) tropical surface waters to the north. These waters are then cooled as they circulate in the NASPG due to a loss of heat to the atmosphere, while they become less salty due to excess local precipitation and freshwater inputs from the Arctic and the ice sheet. The East Greenland Current (EGC) and Labrador Current (LC) are the western branches of the NASPG and carry cold (<4°C) and low-salt (<34.6) waters of polar origin.

Hydrological and biogeochemical properties in the NASPG are impacted by very large variations associated with Atlantic Multi-decadal Variability (AMV), witch result from atmospheric conditions such as the North Atlantic Oscillation (NAO) (Josey et al., 2011; Reverdin, 2010; Robson et al., 2016).

3 Material and Methods

3.1 Data collection and measurements

This study is based on observations collected in the framework of the long-term monitoring program SURATLANT (SURveillance de l'ATLANTique) initiated in 1993. The main objective of this program is to monitor hydrological and biogeochemical properties in surface waters of the NASPG, notably Sea Surface Salinity (SSS) to improve the understanding of the role of salinity on the variability and predictability of climate as well as the water cycle (Reverdin et al., 2018a). To this aim, two to four cruises per year are conducted between Reykjavik (Island) and Newfoundland (Canada) aboard merchant ships. Seawater samples are collected every three to four hours from a pumping system (at approximately 5m deep) in order to measure salinity, as well as Total Alkalinity (TA, measured since 2001), Dissolved Inorganic Carbon (DIC), silicate, nitrate and phosphate concentrations.

Underway measurements of Sea Surface Temperature (SST) are obtained using a Seabird Thermosalinograph, with a precision of 0.10°C. SSS values in this paper are from sample measurements of conductivity using a Guidline AUTOSAL salinometer done since 1997 at the Marine and Freshwater Research Institute (MFRI) in Reykjavik (the associated error is estimated at 0.005). For TA and DIC, the 500 ml glass bottles are rinsed three times before introducing seawater (avoiding introducing air bubbles) with an overflow in order to remove the water in contact with air during filling. The samples are then poisoned with mercuric chloride and stored in a cool, dark place. Since 2001, these samples are measured within three months of collection at the SNAPO-CO_2 (Service National d'Analyse des Paramètres Océaniques du CO_2) located at the Laboratory LOCEAN in Paris. The accuracy is of the order of 3 µmol/kg for both DIC and TA based on CRMs analysis and occasional intercomparisons as explained by Reverdin et al. (2018b). Samples for the analysis of nutrients concentrations are frozen just after sampling. Spring or summer samples are filtered before analysis. The measurement is carried out by the MFRI team in Reykjavik according to the standard colorimetric method described by Olafsson et al. (2010) with an accuracy of 0.2 µmol/l for nitrate and silicate and 0.03 µmol/l for phosphate. Detail of the sampling and analyses for all properties are provided in Reverdin et al. (2018b). The SURATLANT dataset is freely available and is accessible at http://www.seanoe.org/data/00434/54517/.

Biogeosciences Discuss., https://doi.org/10.5194/bg-2019-119
Manuscript under review for journal Biogeosciences
Discussion started: 5 April 2019

3.2 Calculations of the carbonate system parameters and contributions

Carbonate system parameters such as pH, the fugacity of CO_2 (fCO_2) and the saturation states for the calcium carbonate minerals calcite (Ω_{Ca}) and aragonite (Ω_{Ar}) are calculated using measurements of SST, SSS, TA, DIC, silicate and phosphate. For the latter two, we used climatological values derived from the SURATLANT data over the period 1993-2017 because interannual variability does not have a significant impact on the carbonate system parameters calculations (and because sometimes nutrients measurements were not performed). The calculation program used is CO2SYS developed by Lewis et al. (1998) and available for calculations in MS Excel (Pierrot, et al., 2006). The constants of the thermodynamic equilibrium of CO_2 in seawater used are: K1 (for the dissociation of carbonic acid) and K2 (for the bicarbonate ion) defined by Mehrbach et al. (1973), refitted by Dickson and Millero (1987). The total boron value is calculated according to Uppström (1974) and the $KHSO_4$ dissociation constant is from Dickson (1990). The adopted pH scale is total scale.

When TA was not measured (notably before 2001), it was calculated from salinity data. The relationship between sea surface alkalinity and salinity (Eq. 1) was determined by Reverdin et al. (2018) based on all the reported SURATLANT data over the period 2001-2016. This equation was obtained for samples collected north of 50°S with SSS > 34.

$$TA = 45.5337 \times SSS + 713.58\,, \tag{1}$$

Atmospheric fCO_2 values for the period 1993-2017 were calculated from the molar fraction (xCO_2) data at Mace Head provided by the Cooperative Global Atmospheric Data Integration Project (Dlugokencky et al., 2018). The data are available at http://www.esrl.noaa.gov/gmd/dv/iadv/). xCO_2 data were converted to fCO_2 at 100% humidity following Weiss and Price (1980). We did not take into account the interannual variability of surface atmospheric pressure, which can result in small errors on interannual deviations of atmospheric fCO_2.

The trends in sea surface pH, fCO_2, Ω_{Ca} and Ω_{Ar} are driven by changes in SST, SSS, TA and DIC. These contributions are evaluated by allowing a change in only one parameter according to their observed trend, while setting the other parameters to their climatological values (Eq. 2). The contributions uncertainty was evaluated by performing 200 random perturbations within the range of the standard deviation of the observed trends in SST, SSS, TA and DIC.

$$\frac{dX}{dt} = \frac{dX}{dt}\left(\overline{SST}, \overline{SSS}, \overline{TA}, \frac{dDIC}{dt}\right) + \frac{dX}{dt}\left(\overline{SST}, \overline{SSS}, \frac{dTA}{dt}, \overline{DIC}\right) + \frac{dX}{dt}\left(\overline{SST}, \frac{dSSS}{dt}, \overline{TA}, \overline{DIC}\right) + \frac{dX}{dt}\left(\frac{dSST}{dt}, \overline{SSS}, \overline{TA}, \overline{DIC}\right) \tag{2}$$

Here, $\frac{dX}{dt}$ correspond to the trends in pH, fCO_2, Ω_{Ca} and Ω_{Ar} over a given period; and $\overline{SST}, \overline{SSS}, \overline{TA}, \overline{DIC}$ correspond to their climatological values calculated over the same period.

3.3 Data selection

The sampled region was separated into five 4° latitude boxes, according to Reverdin et al. (2018) from 46°N to 64°N (Fig. 2). The southern box (box A: 46°N-50°N) covers the shelf and continental margin of North America and is excluded from this study because of insufficient sampling and large interannual variations due to fresh waters inputs from land and the Arctic. Box B (50°N-54°N) incorporates only samples where SSS is between 34 and 35 (to avoid including continental shelf or NAC waters). For boxes C (54°N-58°N), D (58°N-62°N) and E (62°N-64°N) we used all available data.

Trends during summer (June to August) and winter (January to March) were analyzed separately because these are the seasons corresponding to the extrema in the seasonal cycle (see Sect. 3.1). In addition, they are also the most sampled periods for the SURATLANT surveys (Table 1). Because the seasonal cycle shows month-to-month deviations, we choose February and July as a reference (for winter and summer, respectively). The data collected in January and March (for winter) and in June and August (for summer) were corrected using the month-to-month differences calculated from the climatological cycle.

In order to evaluate the decadal changes within a large region, we combined the data collected between 54°N and 63°N (i.e., boxes C, D and E). The trends in box B are evaluated separately because their DIC and TA values differ from the other three regions.

4 Results

4.1 Seasonal cycle

In order to increase the number of data used in our long-term analysis (because data were not available each year in the reference months February and July, Table 1), we first constructed a monthly climatology for each property and each box, which was used to correct the data collected in January, March, June and August. The mean seasonal cycles constructed from data collected over the period 1993-2017 are portrayed in Fig. 2. SST data (Fig. 2a) show an increase from south to north during winter (5.5°C to 6.8°C), which is not observed during summer (around 12°C in all boxes), while SSS data (Fig. 2b) and TA data (Fig 2.c) show a decrease from south to north, and small seasonal variations. DIC data (Fig. 2d) show much larger seasonal variability than TA, with a maximum in winter due to enhanced vertical mixing, a steep decline from April to May due to phytoplankton blooms, and a minimum at the end of summer. The mean seasonal cycles of fCO_2, pH and Ω (Fig. 2e-h) show fairly similar variations in boxes B, C, D and E. The seasonal changes in fCO_2 and pH are anticorrelated, and the seasonal variability of Ω is relatively similar to that of pH. In all boxes, the maximum in fCO_2 (minimum in pH and Ω) is observed between October and April and related to the maximum in surface DIC, despite the cooling of surface waters. The minimum in fCO_2 (maximum in pH and Ω) is observed during summer (between June and August), and is mainly explained by enhanced primary production, only slightly counterbalanced by sea surface warming.

Biogeosciences Discuss., https://doi.org/10.5194/bg-2019-119
Manuscript under review for journal Biogeosciences
Discussion started: 5 April 2019

4.2 Decadal trends

Figure 3 clearly shows pluriannual trends in hydrological and biogeochemical properties of the NASPG. For this reason, and according to Metzl et al. (2010), the dataset is split into three distinct periods : 1993-1997, 2001-2007 and 2008-2017. Below, we first present the results obtained by combining the boxes C, D and E that are probably more representative of changes in the NASPG than the results in box B that are also influenced by continental inputs.

4.2.1 Trends in region C-D-E

Data collected between 1993 and 1997 show a large increase in surface fCO_2 during summer, accompanied by a sharp decrease in pH and Ω (Fig. 3e-h). This is mainly explained by a rapid increase in SST (Table 2, Fig. 4a, d, g, f). The trend in oceanic fCO_2 (+10.6 µatm/yr) is approximately 5 times faster than the trend in atmospheric fCO_2 (around +2 µatm/yr), which implies important changes in oceanic processes causing a reduction in the summer CO_2 sink over this period. On the opposite, during winter, both hydrological and biogeochemical properties are steady (Fig. 3).

Data collected during the second period (2001-2007) show a large increase in surface fCO_2 during both summer and winter associated with a sharp decrease in pH and Ω (Fig. 3e-h). The trend in oceanic fCO_2 (+11.7 µatm/yr) is about 6 times faster than the trend in atmospheric fCO_2, which implies a reduction in the ability of the ocean to absorb CO_2 from the atmosphere over the period 2001-2007 during both summer and winter. At the end of this period, in winter 2007, oceanic fCO_2 (more than 400 µatm) became higher than atmospheric fCO_2 (around 380 µatm; i.e., the ocean became a source of CO_2 for the atmosphere). Since small trends are observed in SST over this period (Fig. 3a, Table 2), the rapid trends in fCO_2 and pH can be attributed to the increase in DIC and a decrease in TA.

Despite the continuous increase in atmospheric fCO_2 over the last decade (around 2.0 µatm/yr), data collected over the period 2008–2017 show the near-stagnation of surface fCO_2, pH and Ω. As a result, the air-sea CO_2 disequilibrium increased, which means that the ocean was able to absorb more CO_2 from the atmosphere than during the previous periods. In contrast to the previous periods, large interannual variations are observed during summer. Overall, SST, DIC and TA show small or not significant trends over the period 2008-2017 (Table 2).

4.2.2 Trends in region B

The trends in fCO_2, pH and Ω observed in box B show some similarities with those in boxes C, D and E (Fig. 3), but the mechanisms may be different (Fig.4). For example, a rapid increase in fCO_2 (decrease in pH) is also observed in box B during summer over the first period (1993-1997), but it is due to a large increase in DIC rather than warming (Table 2), and as a consequence, it is accompanied by a rapid decrease in Ω (Fig. 3g, h, Table 2). Over the second period (2001-2007), a rapid increase in fCO_2 (decrease in pH and Ω) is observed in all boxes during both summer and winter, mainly explained by an increase in DIC and/or a decrease in TA (depending on the region and season). Over the last period (2008-2017), the trends in fCO_2, pH and Ω in all boxes are smaller than during the previous periods (Table 2). This change in the behavior of the NASPG

appears to be more pronounced in box B during summer with a reversal of the trends (decrease in fCO_2 and increase in pH and Ω).

5 Discussion

Observations collected in the framework of the SURATLANT program show that long-term surface trends in fCO_2 (+1.6 µatm/yr) and pH (-0.0017 /yr) over the period 1993-2017 (Table 2, all boxes, summer and winter) are in the range of the "canonical" views for large-scale surface ocean, generally interpreted by anthropogenic CO_2 uptake, but these trends are not steady and modulated by significant interannual to decadal changes. Depending on the period and season, fCO_2 and pH increase or decrease due to contrasting and competing processes (Fig. 4). Our analysis confirms previous results, such as the rapid fCO_2 increase during winter over the period 2001 – 2007 (Metzl et al., 2010), but this signal is no longer observed over the period 2008-2017. It also highlights significant changes during summer over the period 2001-2007 not previously described. Thereafter we will first discuss the rapid trends observed during summer, then the recent trends observed during winter.

Our observations show remarkable and rapid trends in surface pH and fCO_2 during summer both in 1993-1997 and 2001-2007; which result from competition between SST, DIC and TA changes. Indeed, during the first period, variations in DIC alone (for southern box) and SST (for northern box) are responsible for these trends (Fig.4). This results in a larger coherent regional response. For example, the rapid increase of the DIC in Box B in summer 1993-1997 (+9 µmol/kg/yr) much faster than the anthropogenic signal suggests an increase in productivity at the beginning of the period compared to the end. During the second period, the effect of the TA decrease (potentially related to an advective process or an increase calcification) on fCO_2 and pH is not negligible, as well as the increase in SST and DIC. The trends in pH and fCO_2 presented here are homogeneous spatially during summer and have similar magnitudes than the trends observed during winter. Thus, fCO_2 increased more rapidly in the ocean than in the air, suggesting that the CO_2 sink would have decreased over the period 2001-2007. This period is followed by the near-stagnation of fCO_2 and pH over the last decade (2008-2017). This is concomitant with a strengthening of the winds during some winters, which likely enhanced vertical mixing (Fröb et al., 2018). Trends in hydrological properties show the same sign (summer and winter, north and south), indicating a large-scale behavior. The weak trends in pH and fCO_2 over the last decade deviate from the already published long-term trends (Bates et al., 2014; Lauvset et al., 2015). This result highlights the sensitivity of trends in CO2 uptake and ocean acidification to the sampling period, which must be considered when comparing results with earlier estimates. These different results could be explained by contrasted natural or climate change induced variability in the NASPSS biome having compensating effects, whereas the increase in DIC due to the accumulation of anthropogenic CO_2 is more homogeneous in space. More regional studies are needed to check this hypothesis and to validate estimates obtained by combining data over large regions such as the North Atlantic SubPolar Seasonally Stratified (NASPSS) biome. There is also a need to further investigate the drivers of TA variability, which seem partially decoupled from surface salinity in this part of the North Atlantic subpolar gyre.

To summarize, our observations collected over the last three decades show an abrupt change in the evolution of hydrological and biogeochemical properties in the NASPG around the year 2007. This result is consistent with the studies by Robson et al. (2012, 2016) who reported a rapid warming since the mid-1990s, followed by a cooling by approximately 0.45°C since about 2005. This change is associated with a change in the size of the gyre and increased inputs of subtropical waters from the south (Chafik et al., 2014; Desbruyères et al., 2015), as well as very large heat loss during positive Nord Atlantic Oscillation (NAO) years. Furthermore, the recent study of Landschützer et al. (2019) highlights the dominant role of the Atlantic Multi-decadal Variability (AMV) which transitioned to a positive phase (i.e., warming) in the 1990's (McKinley et al., 2011), and shows a strong correspondence between AMV and thermally driven pCO_2 variations, which can be extrapolated to our study. Indeed, the region investigated in this study (boxes C, D, E) is directly imprinted by NAO (at all periods, according to the NAO index of Jones et al. (1997)) and presents large (AMV)-related multi-decadal SST variability. This result suggests that the uptake of CO_2 could be modulated by NAO with periodicity of nearly 10 years (Nigam et al., 2018), as well as changes in AMV. Fröb et al. (2018) also showed a large increase in DIC (enhanced vertical mixing) during positive NAO conditions (near 60°N, in particular in the Irminger Sea). Along the SURATLANT cruise track, that lies west of the Reykjavik Ridge, the reversal in the SST trend may be slightly delayed (around 2007, Fig. 3a) compared to the basin average. Also the effect of changes in vertical mixing on DIC appears less prominent than further west in Fröb et al. (2018), as it is far from the deep convection areas. However, interannual changes in the nearby Reykjanes Ridge mode waters have been documented (Thierry et al., 2008) that could influence the change in surface DIC.

Another indirect problem of the increase in anthropogenic emissions to the atmosphere is the decrease in the degree of saturation with respect to calcium carbonate (Ω). Because of changes in the trends of the carbonate system parameters, prediction of the time when surface waters will become undersaturated for aragonite and calcite ($\Omega<1$) is highly uncertain. On one hand, when assuming that the slow decrease in Ω observed over the period 2008-2017 will persist in the future (optimistic scenario), undersaturation of surface waters might not be reached in the next 100 years. On the other hand, when considering the average evolution over the last two decades, undersaturation of surface waters could be reached in about 80 years during winter for both aragonite and calcite (30 and 40 years later during summer for aragonite and calcite, respectively).

6 Conclusion and perspectives

The aim of this study was to pursue the study by Metzl et al. (2010) and Reverdin et al. (2018) by evaluating the evolution of the parameters of the carbonate system in surface waters of the NASPG (known as one of the main sinks for anthropogenic CO_2) using data collected over the last three decades, and to better understand the mechanisms responsible for these evolutions. Our study shows a change in the trends around 2007 during both summer and winter for pH and fCO_2, which led to an increase in the ocean capacity to absorb atmospheric CO_2 in the last decade, a near-stagnation of pH and the slowdown of the decline in Ω (carbonate ion concentration) in surface waters. This abrupt change in the evolution of the parameters of the carbonate

system, which could be due to a change in the gyre circulation (inducing changes in the evolution of DIC, SST and TA), followed a period with a rapid increase in fCO_2 and decrease in pH during both summer and winter starting around the year 2001 (this study, Metzl et al., 2010), following a period with a rapid increase in fCO_2 and decrease in pH during summer in the 1990s (this study). Such a multi-decadal variability in hydrological and biogeochemical properties of the NASPG makes it difficult to predict the future evolution of CO_2 uptake and ocean acidification, which advocates for the continuation of long-term monitoring programs in this region. More regional studies are also needed in order to understand the evolution of the parameters of the carbonate system in different areas of the North Atlantic Ocean, where contrasted changes may occur. In addition to ship-based observations, the analysis of data from BGC-Argo floats equipped with pH sensors (together with temperature and salinity sensors, from which TA, DIC and fCO_2 can be estimated) will help to better constrain spatial, seasonal and interannual variability.

Data availability. The data set is freely available and is accessible at http://www.seanoe.org/data/00434/54517/ (http://doi.org/10.17882/54517, Reverdin et al., 2018b).

Author contributions. CL produced the data analyses and wrote the manuscript with inputs from CLM, GR and NM. GR, NM and VR produced the data synthesis. SO provided the nutrients data. JF provided the DIC and TA data.

Competing interests. The authors declare that they have no conflict of interest.

Acknowledgments. The SURATLANT project is supported by the French institute INSU (Institut National des Sciences de l'Univers), the Lamont-Doherty Earth Observatory (LDEO), the National Oceanic and Atmospheric Administration (NOAA) - Atlantic Oceanographic and Meteorological Laboratory (AOML) and the Climate Program Office (CPO). We thank the EIMSKIP Company and the MFRI team, both based in Reykjavik (Iceland), for their cooperation in sea water sampling and analysis. We also thank the numerous scientific volunteers who worked at sea, as well as the crew and captain of the vessels for their help.

References

Bates, N., Astor, Y., Church, M., Currie, K., Dore, J., Gonaález-Dávila, M., Lorenzoni, L., Muller-Karger, F., Olafsson, J. and Santa-Casiano, M.: A Time-Series View of Changing Ocean Chemistry Due to Ocean Uptake of Anthropogenic CO2 and Ocean Acidification, Oceanography, 27(1), 126–141, doi:10.5670/oceanog.2014.16, 2014.

Chafik, L., Rossby, T. and Schrum, C.: On the spatial structure and temporal variability of poleward transport between Scotland and Greenland, Journal of Geophysical Research: Oceans, 119(2), 824–841, doi:10.1002/2013JC009287, 2014.

Corbière, A., Metzl, N., Reverdin, G., Brunet, C. and Takahashi, T.: Interannual and decadal variability of the oceanic carbon sink in the North Atlantic subpolar gyre, Tellus B, 59(2), 168–178, doi:10.1111/j.1600-0889.2006.00232.x, 2007.

Desbruyères, D., Mercier, H. and Thierry, V.: On the mechanisms behind decadal heat content changes in the eastern subpolar gyre, Progress in Oceanography, 132, 262–272, doi:10.1016/j.pocean.2014.02.005, 2015.

Dickson, A. G.: Thermodynamics of the dissociation of boric acid in synthetic seawater from 273.15 to 318.15 K, Deep Sea Research Part A. Oceanographic Research Papers, 37(5), 755–766, doi:10.1016/0198-0149(90)90004-F, 1990.

Dickson, A. G. and Millero, F. J.: A comparison of the equilibrium constants for the dissociation of carbonic acid in seawater media, Deep Sea Research Part A, Oceanographic Research Papers, 34(10), 1733–1743, doi:10.1016/0198-0149(87)90021-5, 1987.

Dlugokencky, E. ., Lang, P. ., Mund, J. ., Crotwell, M. . and Thoning, K. .: Atmospheric Carbon Dioxide Dry Air Mole Fractions from the NOAA ESRL Carbon Cycle Cooperative Global Air Sampling Network, 1968-2017, Version: 2018-07-31,Path: ftp://aftp.cmdl.noaa.gov/data/trace_gases/co2/flask/surface/., 2018.

Doney, S. C., Fabry, V. J., Feely, R. A. and Kleypas, J. A.: Ocean Acidification: The Other CO2 Problem, Annual Review of Marine Science, 1(1), 169–192, doi:10.1146/annurev.marine.010908.163834, 2009.

Fröb, F., Olsen, A., Pérez, F. F., García-Ibáñez, M. I., Jeansson, E., Omar, A. and Lauvset, S. K.: Inorganic carbon and water masses in the Irminger Sea since 1991, Biogeosciences, 15(1), 51–72, doi:https://doi.org/10.5194/bg-15-51-2018, 2018.

Gruber, N., Landschützer, P. and Lovenduski, N. S.: The Variable Southern Ocean Carbon Sink, Annual Review of Marine Science, 11(1), 159–186, doi:10.1146/annurev-marine-121916-063407, 2019.

Hartmann, D.L., A.M.G. Klein Tank, M. Rusticucci, L.V. Alexander, S. Brönnimann, Y. Charabi, F.J. Dentener, E.J. Dlugokencky, D.R. Easterling, A. Kaplan, B.J. Soden, P.W. Thorne, M. Wild and P.M. Zhai.: Observations: Atmosphere and Surface. In: Climate Change 2013: The Physical Science Basis. Contribution of Working Group I to the Fifth Assessment Report of the Intergovernmental Panel on Climate Change [Stocker, T.F., D. Qin, G.-K. Plattner, M. Tignor, S.K. Allen, J. Boschung, A. Nauels, Y. Xia, V. Bex and P.M. Midgley (eds.)]. Cambridge University Press, Cambridge, United Kingdom and New York, NY, USA, pp. 159–254, doi:10.1017/CBO9781107415324.008, 2013.

Jones, P. D., Jonsson, T. and Wheeler, D. A.: Monthly values of the North Atlantic Oscillation Index from 1821 to 2000, Supplement to: Jones, PD et al. (1997): Extension to the North Atlantic Oscillation using early instrumental pressure observations from Gibraltar and South-West Iceland. International Journal of Climatology, 17(13), 1433-1450, https://doi.org/10.1002/(SICI)1097-0088(19971115)17:13%3C1433::AID-JOC203%3E3.0.CO;2-P, doi:https://doi.org/10.1594/PANGAEA.56559, 1997.

Josey, S. A., Somot, S. and Tsimplis, M.: Impacts of atmospheric modes of variability on Mediterranean Sea surface heat exchange, Journal of Geophysical Research: Oceans, 116(C2), doi:10.1029/2010JC006685, 2011.

Khatiwala, S., Tanhua, T., Mikaloff Fletcher, S., Gerber, M., Doney, S. C., Graven, H. D., Gruber, N., McKinley, G. A., Murata, A., Ríos, A. F. and Sabine, C. L.: Global ocean storage of anthropogenic carbon, Biogeosciences, 10(4), 2169–2191, doi:https://doi.org/10.5194/bg-10-2169-2013, 2013.

Landschützer, P., Gruber, N., Bakker, D. C. E., Schuster, U., Nakaoka, S., Payne, M. R., Sasse, T. P. and Zeng, J.: A neural network-based estimate of the seasonal to inter-annual variability of the Atlantic Ocean carbon sink, , 23, 2013.

Landschützer, P., Ilyina, T. and Lovenduski, N. S.: Detecting Regional Modes of Variability in Observation-Based Surface Ocean pCO2, Geophysical Research Letters, 0(0), doi:10.1029/2018GL081756, 2019.

Lauvset, S. K. and Gruber, N.: Long-term trends in surface ocean pH in the North Atlantic, 0304-4203, doi:10.1016/j.marchem.2014.03.009, 2014.

Lauvset, S. K., Gruber, N., Landschützer, P., Olsen, A. and Tjiputra, J.: Trends and drivers in global surface ocean pH over the past 3 decades, Biogeosciences, 12(5), 1285–1298, doi:10.5194/bg-12-1285-2015, 2015.

Le Quéré, C., Andrew, R. M., Friedlingstein, P., Sitch, S., Hauck, J., Pongratz, J., Pickers, P. A., Korsbakken, J. I., Peters, G. P., Canadell, J. G., Arneth, A., Arora, V. K., Barbero, L., Bastos, A., Bopp, L., Chevallier, F., Chini, L. P., Ciais, P., Doney, S. C., Gkritzalis, T., Goll, D. S., Harris, I., Haverd, V., Hoffman, F. M., Hoppema, M., Houghton, R. A., Hurtt, G., Ilyina, T., Jain, A. K., Johannessen, T., Jones, C. D., Kato, E., Keeling, R. F., Goldewijk, K. K., Landschützer, P., Lefèvre, N., Lienert, S., Liu, Z., Lombardozzi, D., Metzl, N., Munro, D. R., Nabel, J. E. M. S., Nakaoka, S., Neill, C., Olsen, A., Ono, T., Patra, P., Peregon, A., Peters, W., Peylin, P., Pfeil, B., Pierrot, D., Poulter, B., Rehder, G., Resplandy, L., Robertson, E., Rocher, M., Rödenbeck, C., Schuster, U., Schwinger, J., Séférian, R., Skjelvan, I., Steinhoff, T., Sutton, A., Tans, P. P., Tian, H., Tilbrook, B., Tubiello, F. N., Laan-Luijkx, I. T. van der, Werf, G. R. van der, Viovy, N., Walker, A. P., Wiltshire, A. J., Wright, R., Zaehle, S. and Zheng, B.: Global Carbon Budget 2018, Earth System Science Data, 10(4), 2141–2194, doi:https://doi.org/10.5194/essd-10-2141-2018, 2018.

Lewis, E., Wallace, D. and Allison, L. J.: Program developed for CO2 system calculations, Brookhaven National Lab., Dept. of Applied Science, Upton, NY (United States); Oak Ridge National Lab., Carbon Dioxide Information Analysis Center, TN (United States)., 1998.

McKinley, G. A., Fay, A. R., Takahashi, T. and Metzl, N.: Convergence of atmospheric and North Atlantic carbon dioxide trends on multidecadal timescales, Nature Geoscience, 4(9), 606–610, doi:10.1038/ngeo1193, 2011.

Mehrbach, C., Culberson, C. H., Hawley, J. E. and Pytkowicx, R. M.: Measurement of the Apparent Dissociation Constants of Carbonic Acid in Seawater at Atmospheric Pressure1, Limnology and Oceanography, 18(6), 897–907, doi:10.4319/lo.1973.18.6.0897, 1973.

Metzl, N., Corbière, A., Reverdin, G., Lenton, A., Takahashi, T., Olsen, A., Johannessen, T., Pierrot, D., Wanninkhof, R., Ólafsdóttir, S. R., Olafsson, J. and Ramonet, M.: Recent acceleration of the sea surface fCO2 growth rate in the North Atlantic subpolar gyre (1993–2008) revealed by winter observations, Global Biogeochemical Cycles, 24(4), doi:10.1029/2009GB003658, 2010.

Nigam, S., Ruiz-Barradas, A. and Chafik, L.: Gulf Stream Excursions and Sectional Detachments Generate the Decadal Pulses in the Atlantic Multidecadal Oscillation, Journal of Climate, 31(7), 2853–2870, doi:10.1175/JCLI-D-17-0010.1, 2018.

Ólafsson, J., Ólafsdóttir, S. R., Benoit-Cattin, A. and Takahashi, T.: Hydrochemistry measured on water bottle samples during Bjarni Saemundsson cruise B11/2004, In supplement to: Ólafsson, J et al. (2010): The Irminger Sea and the Iceland Sea time series measurements of sea water carbon and nutrient chemistry 1983–2006. Earth System Science Data, 2(1), 99-104, https://doi.org/10.5194/essd-2-99-2010, doi:https://doi.org/10.1594/PANGAEA.774097, 2010.

World Meteorological Organization (WMO), W. M., (UNESCO) United Nations Educational, S. and C. O., Commission, (IOC) Intergovernmental Oceanographic, Programme, (UNEP) United Nations Environment, Science, (ICSU) International Council for, Climate (OOPC-21), 21st Session of the Ocean Observations Panel for and World Meteorological Organization (WMO): GCOS, 217. 21st Session of the Ocean Observations Panel for Climate (the GOOS Physics and Climate Panel) (OOPC-21), WMO., 2018.

Pierrot, D. E., Wallace, D. W. R. and Lewis, E.: MS Excel Program Developed for CO2 System Calculations, Carbon Dioxide Information Analysis Center, Oak Ridge National Laboratory, U.S. Department of Energy, Oak Ridge, Tennessee, doi:10.3334/CDIAC/otg.CO2SYS_XLS_CDIAC105a, 2006.

Reverdin, G.: North Atlantic Subpolar Gyre Surface Variability (1895–2009), J. Climate, 23(17), 4571–4584, doi:10.1175/2010JCLI3493.1, 2010.

Reverdin, G., Valdimarsson, H., Alory, G., Diverres, D., Bringas, F., Goni, G., Heilmann, L., Chafik, L., Szekely, T. and Friedman, A. R.: North Atlantic subpolar gyre along predetermined ship tracks since 1993: a monthly data set of surface temperature, salinity, and density, Earth System Science Data, 10(3), 1403–1415, doi:https://doi.org/10.5194/essd-10-1403-2018, 2018a.

Reverdin, G., Metzl, N., Olafsdottir, S., Racapé, V., Takahashi, T., Benetti, M., Valdimarsson, H., Benoit-Cattin, A., Danielsen, M., Fin, J., Naamar, A., Pierrot, D., Sullivan, K., Bringas, F. and Goni, G.: SURATLANT: a 1993–2017 surface sampling in the central part of the North Atlantic subpolar gyre, Earth System Science Data, 10(4), 1901–1924, doi:10.5194/essd-10-1901-2018, 2018b.

Robson, J., Sutton, R., Lohmann, K., Smith, D. and Palmer, M. D.: Causes of the Rapid Warming of the North Atlantic Ocean in the Mid-1990s, J. Climate, 25(12), 4116–4134, doi:10.1175/JCLI-D-11-00443.1, 2012.

Robson, J., Ortega, P. and Sutton, R.: A reversal of climatic trends in the North Atlantic since 2005, Nature Geoscience, 9(7), 513–517, doi:10.1038/ngeo2727, 2016.

Sabine, C. L., Feely, R. A., Gruber, N., Key, R. M., Lee, K., Bullister, J. L., Wanninkhof, R., Wong, C. S., Wallace, D. W. R., Tilbrook, B., Millero, F. J., Peng, T.-H., Kozyr, A., Ono, T. and Rios, A. F.: The Oceanic Sink for Anthropogenic CO2, Science, 305(5682), 367–371, doi:10.1126/science.1097403, 2004.

Takahashi, T., Sutherland, S. C., Wanninkhof, R., Sweeney, C., Feely, R. A., Chipman, D. W., Hales, B., Friederich, G., Chavez, F., Sabine, C., Watson, A., Bakker, D. C. E., Schuster, U., Metzl, N., Yoshikawa-Inoue, H., Ishii, M., Midorikawa, T., Nojiri, Y., Körtzinger, A., Steinhoff, T., Hoppema, M., Olafsson, J., Arnarson, T. S., Tilbrook, B., Johannessen, T., Olsen, A., Bellerby, R., Wong, C. S., Delille, B., Bates, N. R. and de Baar, H. J. W.: Climatological mean and decadal change in surface ocean pCO2, and net sea–air CO2 flux over the global oceans, Deep Sea Research Part II: Topical Studies in Oceanography, 56(8–10), 554–577, doi:10.1016/j.dsr2.2008.12.009, 2009.

Thierry, V., Boisséson, E. de and Mercier, H.: Interannual variability of the Subpolar Mode Water properties over the Reykjanes Ridge during 1990–2006, Journal of Geophysical Research: Oceans, 113(C4), doi:10.1029/2007JC004443, 2008.

Uppström, L. R.: The boron/chlorinity ratio of deep-sea water from the Pacific Ocean, Deep Sea Research and Oceanographic Abstracts, 21, 161–162, doi:10.1016/0011-7471(74)90074-6, 1974.

Weiss, R. F. and Price, B. A.: Nitrous oxide solubility in water and seawater, Marine Chemistry, 8(4), 347–359, doi:10.1016/0304-4203(80)90024-9, 1980.

Biogeosciences Discuss., https://doi.org/10.5194/bg-2019-119
Manuscript under review for journal Biogeosciences
Discussion started: 5 April 2019

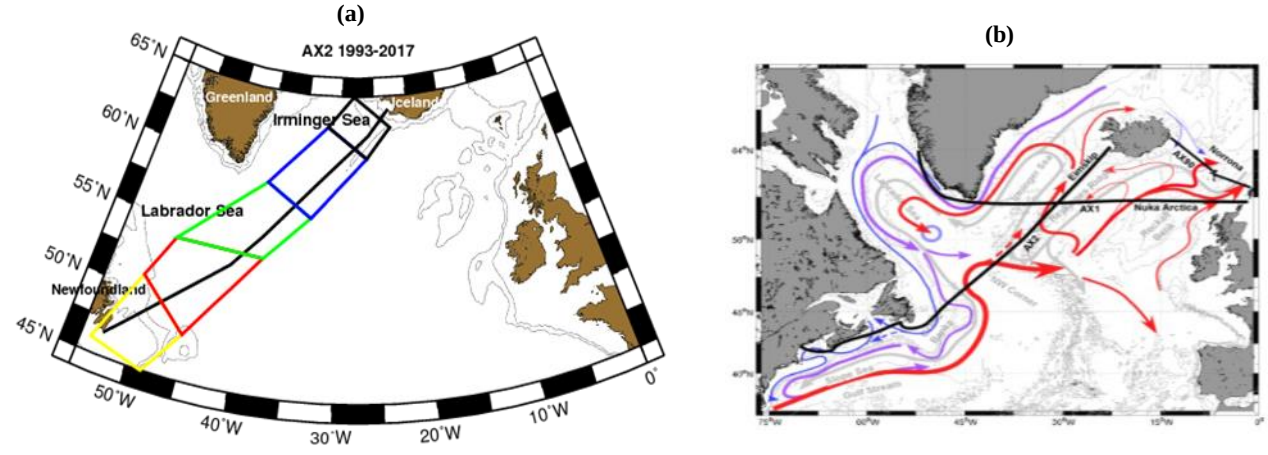

Figure 1. SURATLANT cruises track (in black, AX2 on panel b) with **a)** the five boxes [Box A : 46°N-50°N (in yellow), Box B : 50°N-54°N (in red), Box C : 54°N-58°N (in green), Box D : 58°N-62°N (in blue) and Box E : 62°N-64°N (in black)] and **b)** surface currents in the North Atlantic Subpolar Gyre (NASPG). The NASPG circulation (resulting from the Gulf Stream and the North Atlantic Current) is shown in red, fresher waters of polar or continental origins are shown in blue, and the export of surface waters to depth is shown in purple (figures from Reverdin et al., 2018b)

Biogeosciences Discuss., https://doi.org/10.5194/bg-2019-119
Manuscript under review for journal Biogeosciences
Discussion started: 5 April 2019

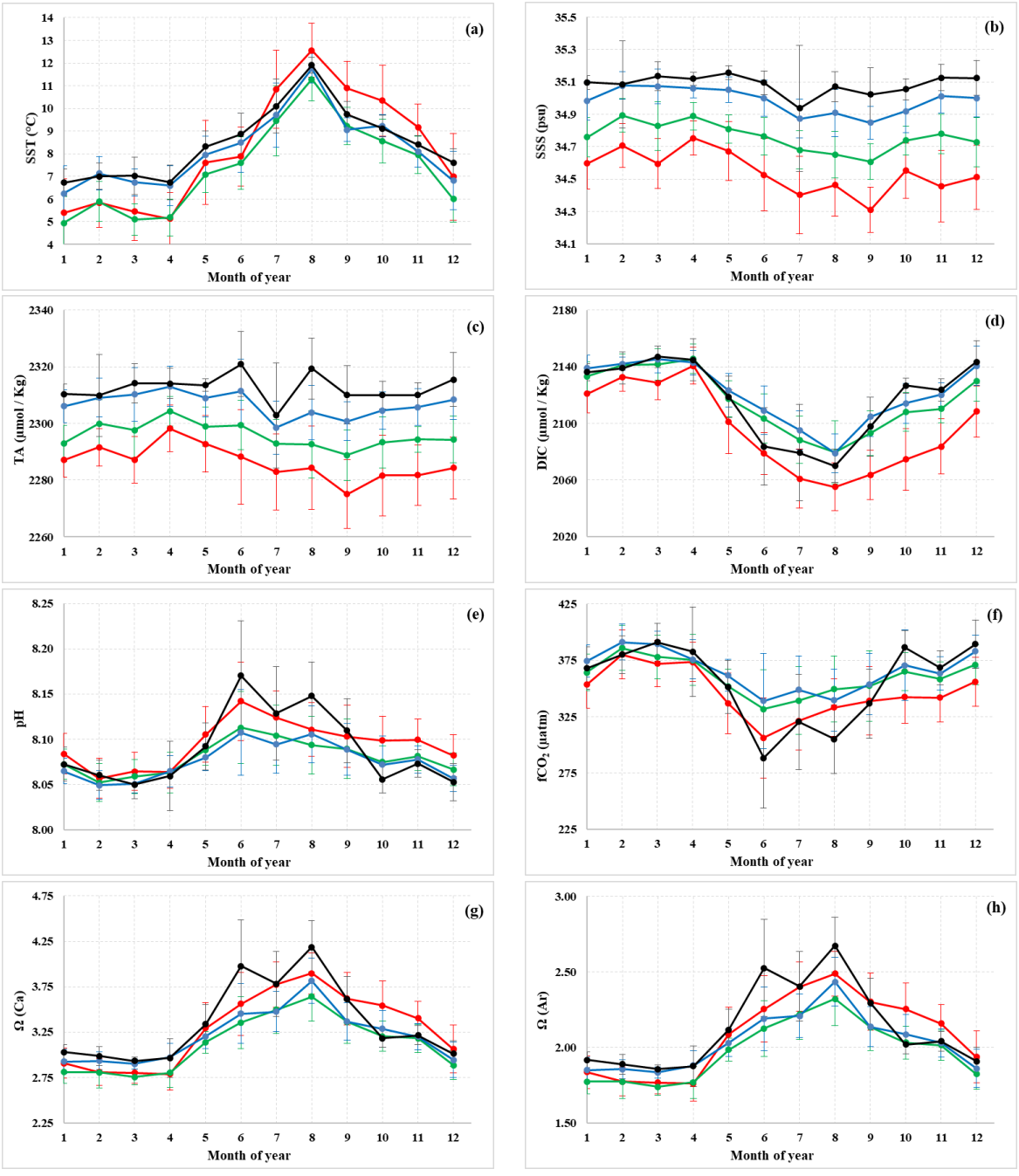

Figure 2. Mean seasonal cycles of **a)** SST, **b)** SSS, **c)** TA, **d)** DIC, **e)** pH, **f)** fCO_2, **g)** Ω_{Ca} and **h)** Ω_{Ar} over the period 1993-2017 in the boxes B, C, D and E identified with corresponding colors in Figure 1a (panel d, Reverdin et al., 2018). Errors bars result from both interannual and spatial variability within a box.

Biogeosciences Discuss., https://doi.org/10.5194/bg-2019-119
Manuscript under review for journal Biogeosciences
Discussion started: 5 April 2019

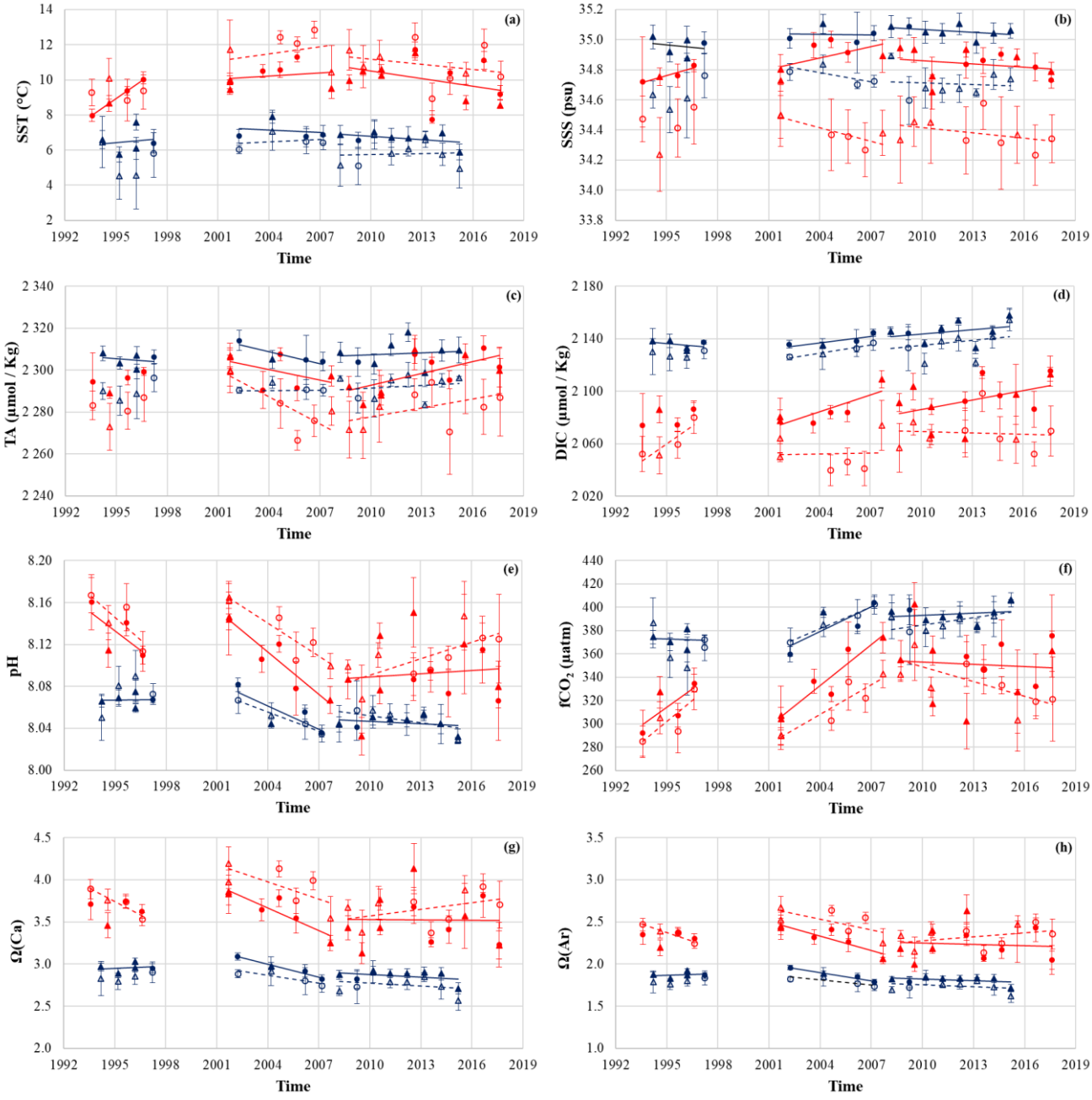

Figure 3. Evolution of **a)** SST, **b)** SSS, **c)** TA, **d)** DIC, **e)** pH, **f)** fCO_2, **g)** Ω_{Ca} and **h)** Ω_{Ar} between 1993 and 2017, are obtained in box B (open symbols) and by combining all data in boxes C, D, E (filled symbols) during summer (in red) and during winter (in blue). Data from February and July are indicated with circles and the reconstructed data are depicted with triangles. Only trends whose error is below a defined threshold are represented with dash lines (for box B) and solid lines (for boxes C, D, E). The thresholds are: ±0.12 °C/yr (SST), ±0.03 psu/yr (SSS), ±1.0 µmol/kg/yr (TA), ±1.5 µmol/kg/yr (DIC), ±0.0032 /yr (pH), ±2.5 µatm/yr (fCO_2), ±0.020 /yr (Ω_{Ca}) and ±0.013 /yr (Ω_{Ar}).

Biogeosciences Discuss., https://doi.org/10.5194/bg-2019-119
Manuscript under review for journal Biogeosciences
Discussion started: 5 April 2019

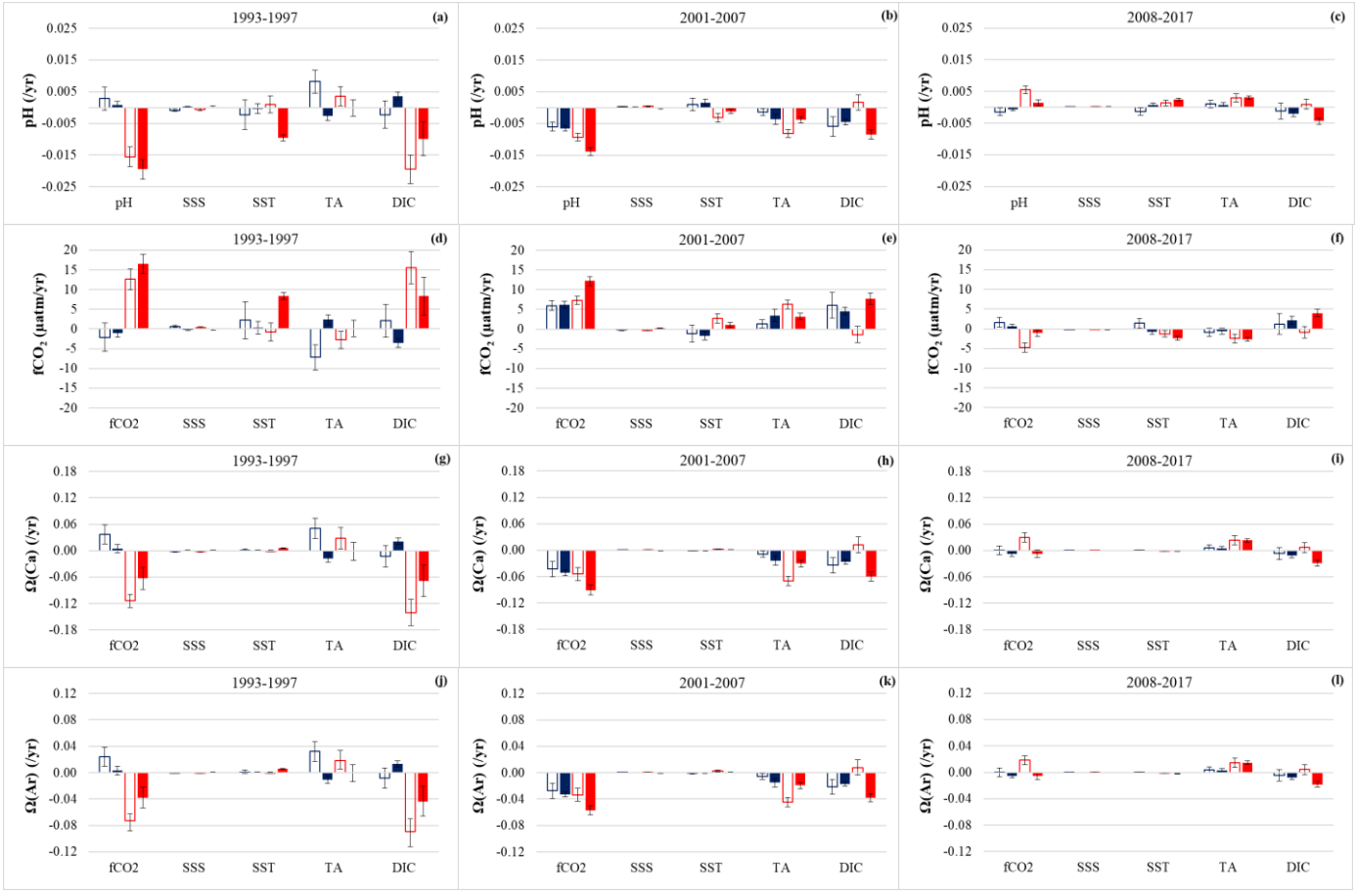

Figure 4. Decomposition of the trends in surface pH (a-c), fCO_2 (d-f), Ω_{Ca} (g-i) and Ω_{Ar} (j-l). The effect of the changes in SSS, SST, TA and DIC is shown for the three periods: 1993-1997 (left column), 2001-2007 (middle column) and 2008-2017 (right column). Color coding is the same as in Figure 3.

Biogeosciences Discuss., https://doi.org/10.5194/bg-2019-119
Manuscript under review for journal Biogeosciences
Discussion started: 5 April 2019

Table 1. SURATLANT sampling since 1993 for each box in Figure 1a.

	Jan	Feb	Mar	Apr	May	Jun	Jul	Aug	Sep	Oct	Nov	Dec
1993							A-B-C-D-E					
1994	A-B-C-D-E			A-B-C-D-E		A-B-C-D-E			A-B-C-D-E			
1995	A-B-C-D-E				A-B-C-D-E		A-B-C-D-E					A-B-C
1996	C-D-E		A-B-C-D-E				A-B-C-D-E					
1997		A-B-C-D-E										
2001						A-B-C-D-E		A-B-C-D-E				A-B-C-D-E
2002		A-B-C-D-E			A-B-C-D-E				A-B-C-D-E			A-B-C-D
2003				A-B-C-D-E			A-B-C-D-E			B-C-D-E		
2004	B-C-D-E				B-C-D-E		A-B-C-D-E				B-C-D-E	
2005					A-B-C-D-E	A	A-B-C-D-E				B-C-D-E	
2006		B-C-D-E			A-B-C-D-E		A-B-C				A-B-C-D-E	
2007		B-C-D-E						A-B-C-D-E		A-B-C-D-E		
2008			A-B-C-D-E		B-C-D-E		B	C-D-E			A-B-C-D-E	
2009		A-B-C-D-E				A-B-C-D-E			B-C-D-E			A-B-C-D-E
2010			B-C-D-E			A-B-C-D-E		A-B-C-D-E				A-B-C-D-E
2011			B-C-D-E									B-C-D-E
2012			A-B-C-D-E			E	A-B-C-D-E		A-B-C-D-E			A-B-C-D
2013			B-C-D-E				A-B-C-D-E		B-C-D-E	A		
2014	A-B-C-D-E			B-C-D-E			A-B-C-D-E			A-B-C-D-E		
2015	A-B-C-D-E					A-B-C-D-E			A-B-C-D-E			A-B-C-D-E
2016				A-B-C-D-E			A-B-C-D-E			B-C-D-E		
2017							B-C-D-E	C-D				

Table 2. Trends (per year) evaluated from data presented in Figure 3.

		box	SST (°C/yr)	SSS (/yr)	TA (µmol/kg/yr)	DIC (µmol/kg/yr)	pH (/yr)	fCO2 (µatm/yr)	Ωca (/yr)	Ωar (/yr)
1993-1997	summer	B	-0.10 ±0.16	0.041 ±0.034	1.8 ±1.6	**9.0 ±2***	**-0.0143 ±0.0031***	**12.0 ±2.6***	**-0.107 ±0.015***	**-0.069 ±0.01***
		C.D.E	**0.68 ±0.06***	**0.032 ±0.028**	2.2 ±1.3	2.4 ±2.3	**-0.0123 ±0.0031***	**10.6 ±2.4***	0.005 ±0.025*	-0.069 ±0.016*
	winter	B	-0.19 ±0.3	0.045 ±0.032	2.2 ±1.5	0.1 ±1.8	0.0075 ±0.0037	-7.2 ±3.6	0.028 ±0.022	0.017 ±0.015
		C.D.E	**0.09 ±0.1**	**-0.011 ±0.015**	**-0.6 ±0.6**	**-1.2 ±0.5***	**0.0002 ±0.001**	**-0.4 ±1**	**0.009 ±0.01**	**0.006 ±0.006**
2001-2007	summer	B	**0.13 ±0.09**	**-0.030 ±0.013***	**-4.3 ±0.7***	**0.2 ±1.2**	**-0.0105 ±0.0012***	**8.5 ±1***	**-0.068 ±0.015***	**-0.043 ±0.01***
		C. D. E	**0.06 ±0.04**	**0.025 ±0.008***	**-1.7 ±0.5***	**4.3 ±0.7***	**-0.0134 ±0.0013***	**11.7 ±1.1***	**-0.090 ±0.011***	**-0.057 ±0.007***
	winter	B	**0.04 ±0.11**	**-0.020 ±0.008***	**-0.2 ±0.4**	**2.1 ±1.2**	**-0.0061 ±0.0014***	**6.2 ±1.3***	**-0.031 ±0.018**	**-0.020 ±0.011**
		C. D. E	**-0.05 ±0.07**	**-0.002 ±0.012**	**-1.9 ±0.7***	**1.6 ±0.4***	**-0.0074 ±0.0009***	**7.0 ±0.9***	**-0.051 ±0.006***	**-0.032 ±0.004***
2008-2017	summer	B	**-0.10 ±0.06**	**-0.012 ±0.009**	**1.4 ±0.7**	**-0.3 ±0.8**	**0.0052 ±0.0013***	**-4.3 ±1.1***	**0.026 ±0.011***	**0.016 ±0.007***
		C. D. E	**-0.14 ±0.03***	**-0.007 ±0.004***	**1.9 ±0.3***	**2.4 ±0.5***	**0.0010 ±0.001**	**-0.6 ±0.8**	**-0.007 ±0.008**	**-0.005 ±0.005**
	winter	B	**0.02 ±0.07**	**-0.004 ±0.009**	**0.4 ±0.5**	**1.3 ±0.9**	**-0.0023 ±0.0012**	**2.2 ±1.2**	**-0.011 ±0.01**	**-0.007 ±0.006**
		C. D. E	**-0.07 ±0.04**	**-0.007 ±0.005**	**0.3 ±0.4**	**1.1 ±0.4***	**-0.0007 ±0.0005**	**0.6 ±0.5**	**-0.011 ±0.005**	**-0.007 ±0.003**
1993-2017	summer	B	**0.06 ±0.02***	**-0.004 ±0.002**	**0.0 ±0.2**	**0.4 ±0.2**	**-0.0017 ±0.0004***	**1.5 ±0.3***	**-0.005 ±0.003**	**-0.003 ±0.002**
		C.D.E	**0.03 ±0.01***	**0.003 ±0.001***	**0.2 ±0.1***	**1.0 ±0.1***	**-0.0022 ±0.0003***	**2.0 ±0.2***	**-0.011 ±0.002***	**-0.007 ±0.001***
		B. C. D. E	**0.04 ±0.01***	**0.001 ±0.002**	**0.2 ±0.1**	**0.9 ±0.1***	**-0.0021 ±0.0002***	**1.9 ±0.2***	**-0.010 ±0.002***	**-0.006 ±0.001***
	winter	B	**0.04 ±0.02**	**0.004 ±0.002**	**0.1 ±0.1**	**0.5 ±0.2***	**-0.0017 ±0.0003***	**1.7 ±0.3***	**-0.006 ±0.002**	**-0.003 ±0.001**
		C.D.E	**0.02 ±0.01***	**0.006 ±0.001***	**0.1 ±0.1***	**0.6 ±0.1***	**-0.0016 ±0.0001***	**1.6 ±0.1***	**-0.007 ±0.001***	**-0.004 ±0.001***
		B. C. D. E	**0.02 ±0.01***	**0.005 ±0.001***	**0.1 ±0.1**	**0.6 ±0.1***	**-0.0016 ±0.0001***	**1.6 ±0.1***	**-0.006 ±0.001***	**-0.004 ±0.001***

* Significant trends (Student test).

In bold, the trends with small errors (criteria according to Figure 3).